Electronic Supplementary Material (ESI) for Sustainable Energy & Fuels.

Supporting Information

Effective Solar-Light-Driven Photocatalytic Production of Hypobromous Acid on Film-Like Photocatalyst Sheets

Rui Pang,[a] Yugo Miseki,[a] and Kazuhiro Sayama*[a]

*Corresponding Author: Fax: +81-29-861-4760; Tel: +81-29-6234. Email: k.sayama@aist.go.jp.

[a] Artificial Photosynthesis Research Team, Global Zero Emission Research Center, National Institute of Advanced Industrial Science and Technology, Tsukuba West, 16-1, Onogawa, Tsukuba, Ibaraki, 305-0053, Japan.

1S. Experimental

1.1S Electrochemical measurement

Oxidative photoelectrochemical HBrO production was performed under solar light using the as-prepared $BiVO_4/WO_3$/FTO photoelectrode with a two-electrode system in a one-compartment cell. $BiVO_4/WO_3$/FTO and Pt/FTO electrodes worked as the working and counter electrodes, respectively. Gaseous O_2 was bubbled in 100 mL of 0.5 M aqueous solution of NaBr at a flow rate of 1 mL min^{-1}. The photoelectrochemical reaction was carried out under the photoirradiation of simulated solar light (irradiation area: 6.0 cm^2). The HBrO concentration produced in the analyte solution was determined utilising the DPD method and calculated using **Eq. 1**. The faradaic efficiency of HBrO (FE_{HBrO}) production in 100 mL of the electrolyte solution was calculated using **Eq. S1**:

$$FE_{HBrO} = 100 \times (2 \times C_{HBrO} \times 0.1)/(C/F) \quad \text{(S1)}$$

where C and F denote the electric charge and Faraday constant, respectively.

The production of HBrO at the $BiVO_4/WO_3$/FTO photoanode and the production of H_2O_2 at the Pt/FTO cathode were carried out using a two-compartment cell with an aqueous NaBr solution as the electrolyte (0.5 M, 35 mL). The photocathode chamber was separated by an ion-exchange membrane (SELEMION, AGC Engineering Co., Ltd.)

with an anode chamber. Gaseous O_2 was bubbled into the cathode chambers at a flow rate of 1 mL min^{-1}. The $BiVO_4/WO_3$/FTO photoanode was illuminated under simulated solar light, and no bias was added during the photoelectrochemical reaction. After photoirradiation for 30 min, the concentration of HBrO produced in the anode chamber solution was measured using the DPD method, as mentioned earlier. The H_2O_2 concentration (C_{H2O2}) produced in the cathode chamber solution was measured using the DPD method in the presence of peroxidase (Oriental Yeast Co., Ltd.)[1] and calculated according to **Eq. S2**:

$$C_{H2O2} = Abs_{552}/0.00225\ (\mu M) \quad (S2)$$

The electrochemical impedance spectroscopy (EIS) of WO_3/FTO, $BiVO_4$/FTO, and $BiVO_4/WO_3$/FTO photoelectrodes was performed in 0.5 M NaBr electrolyte at 0 V *vs.* RHE under AM 1.5 illumination in a one-chamber compartment cell without an ion-exchange membrane. Photocatalyst/FTO, Ag/AgCl, and Pt wire were used as working, reference, and counter electrodes, respectively.

1.2S Apparent quantum yield measurement

The apparent quantum yield (AQY) of HBrO formation during the photocatalytic oxidation of Br^- over the Pt–$BiVO_4/WO_3$/FTO photocatalyst sheet was measured with monochromatic light through a bandpass filter (Asahi Spectra Co, MAX-302) under

identical reaction conditions. The AQY value can be calculated using **Eq. S3**:

$$\text{AQY} = \frac{2 \times C(\text{HBrO}) \times n}{N} \times 100\% \quad \text{(S3)}$$

where *C*(HBrO), *n* and *N* denote the concentration of HBrO produced, the number of molecules per molar (6.02×10^{23} mol^{-1}) and the number of incident photons, respectively. *N* was calculated from **Eq. S4**:

$$\text{N} = \frac{E_\lambda}{E_0} = \frac{E_\lambda \times \lambda}{h \times \text{c}} = \frac{\text{P} \times \text{S} \times \text{t} \times \lambda}{h \times \text{c}} \quad \text{(S4)}$$

where E_λ, E_0, *P*, *S*, *t*, λ, *h* and *c* denote the incident energy, the energy of each photons ($E_0 = hv = hc/\lambda$), the intensity of irradiation measured using a digital multimeter (Advantest, AD7451A), the irradiated area (9.0 cm^2), the irradiation time (3,600 s), the wavelength of light, Plank's constant (6.63×10^{-34} J·s) and the speed of light (3.0×10^8 m s^{-1}), respectively.

1.3S Photocurrent density measurement

The current–time (*I*–*t*) curve of the oxidative photoelectrochemical HBrO production over $BiVO_4$/FTO, WO_3/FTO and $BiVO_4$/WO_3/FTO photoanodes (irradiation area: 6 cm^2) was performed with a three-electrode system using a one-compartment cell under simulated solar light irradiation. Photocatalyst/FTO-, silver/silver-chloride- and Pt-wire electrodes worked as the working, reference and counter electrodes, respectively. Gaseous O_2 was bubbled in 100 mL of 0.5 M aqueous solution of NaBr at a flow rate of

1 mL min^{-1}. No external bias was added during scanning for 1,800 s.

References

1. Bader, H.; Sturzenegger, V.; Hoigne, J., *Water Res.* 1988**, 22***,* 1109-1115.

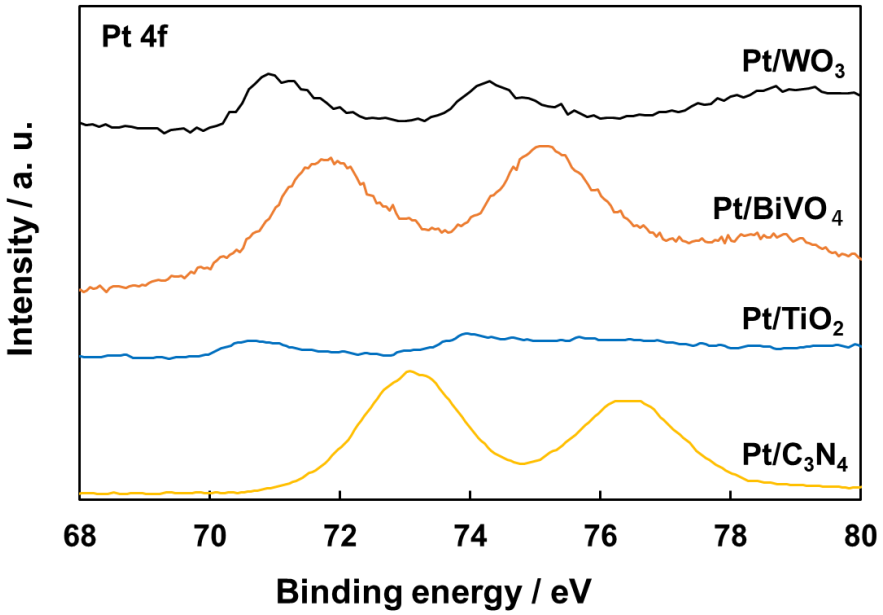

Fig. S1. XPS spectra of Pt 4f in various Pt/photocatalysts.

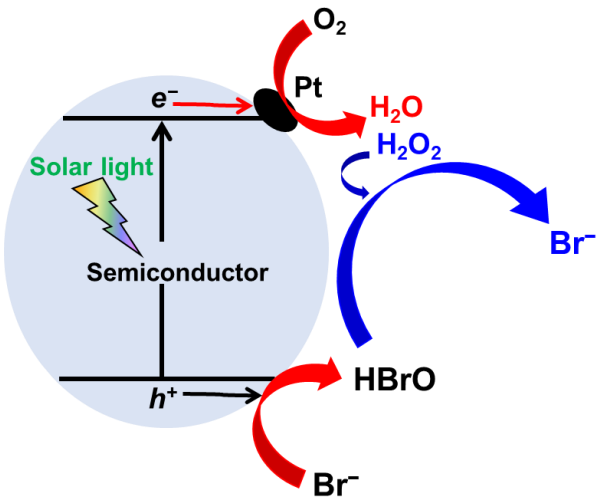

Fig. S2. Schematic illustration of reaction mechanism for the production and accumulation of HBrO over the Pt/semiconductor photocatalyst under solar light irradiation.

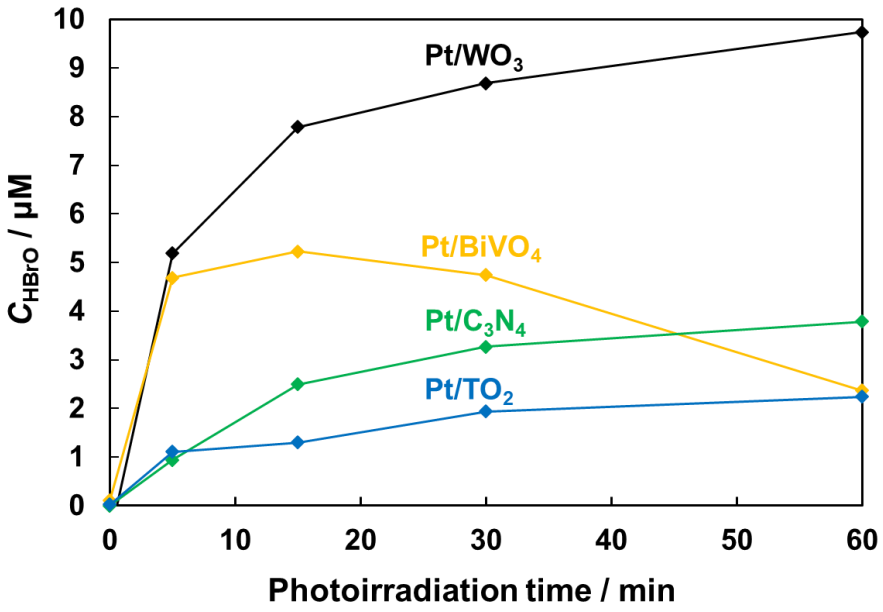

Fig. S3. The concentration of HBrO produced over the Pt/WO_3, $Pt/BiVO_4$, Pt/C_3N_4 and Pt/TiO_2 photocatalysts in an aqueous solution of NaBr under simulated solar light for 60 min. Photocatalyst amount: 50 mg; Pt cocatalyst amount: 1.0 wt% of photocatalyst; reaction solution: 0.5 M NaBr, 50 mL; O_2 flow rate: 1 mL min^{-1}; light source: simulated solar light (AM-1.5, 1 SUN); irradiation area: approximately 20 cm^2; temperature: 303 K.

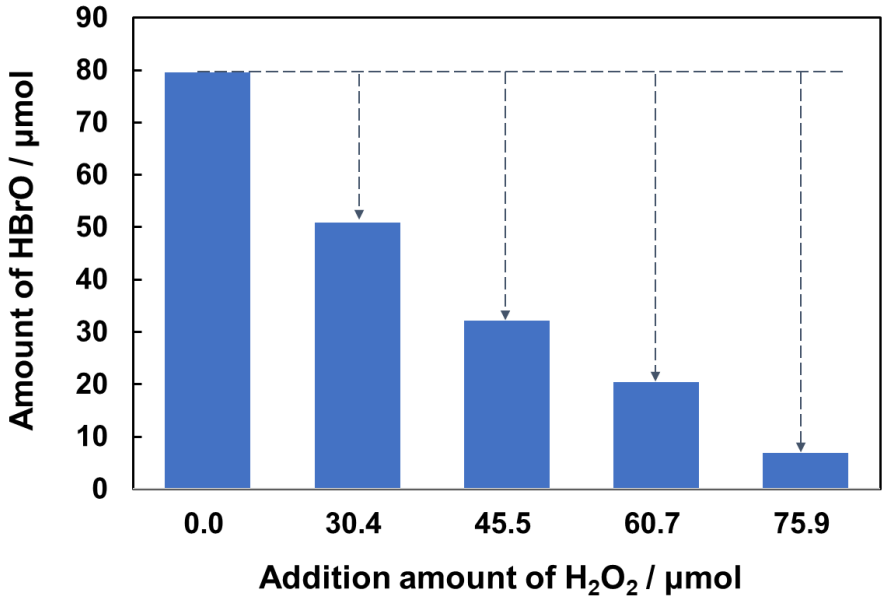

Fig. S4. Amount of HBrO after adding various amount of H_2O_2 under dark condition. The initial amount of HBrO was ~80 µmol, total volume of solution was 10 mL.

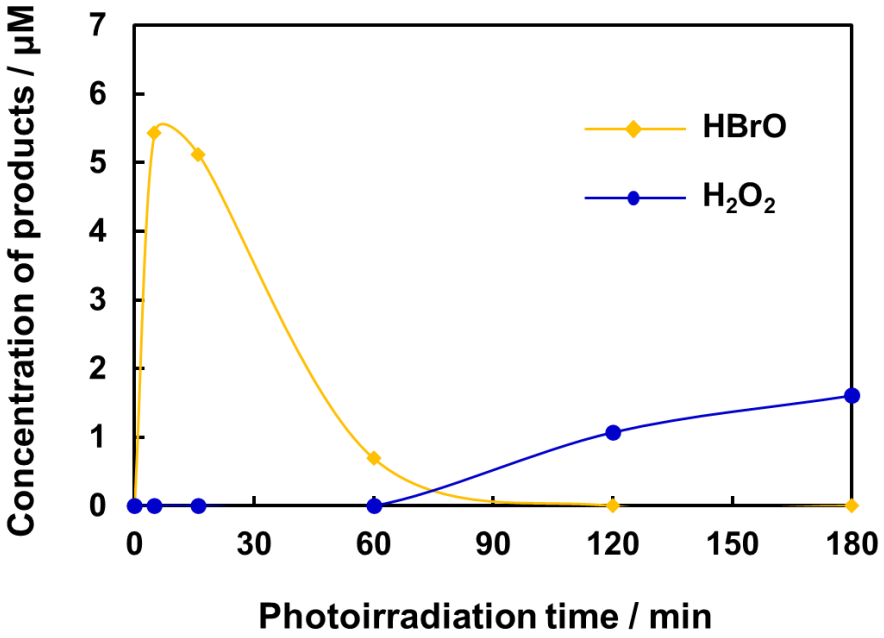

Fig. S5. The concentration of HBrO and H_2O_2 produced over the Pt/$BiVO_4$ in an aqueous solution of NaBr under simulated solar light for 180 min. Photocatalyst amount: 50 mg; Pt cocatalyst amount: 1.0 wt% of photocatalyst; reaction solution: 0.5 M NaBr, 50 mL; O_2 flow rate: 1 mL min^{-1}; light source: simulated solar light (AM-1.5, 1 SUN); irradiation area: approximately 20 cm^2; temperature: 303 K.

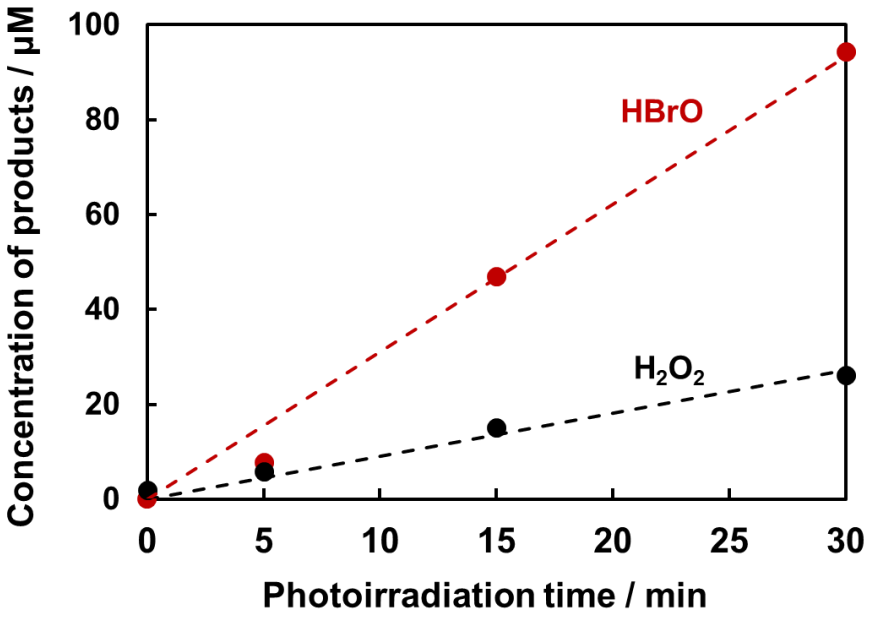

Fig. S6. Concentration of HBrO produced on the $BiVO_4/WO_3$/FTO photoanode and H_2O_2 produced on the Pt/FTO cathode in a two-compartment cell without applied voltage under solar light irradiation. System: two-electrode system; electrolyte: 0.5 M NaBr aqueous solution, 35 mL; light source: simulated solar light (AM-1.5, 1 SUN).

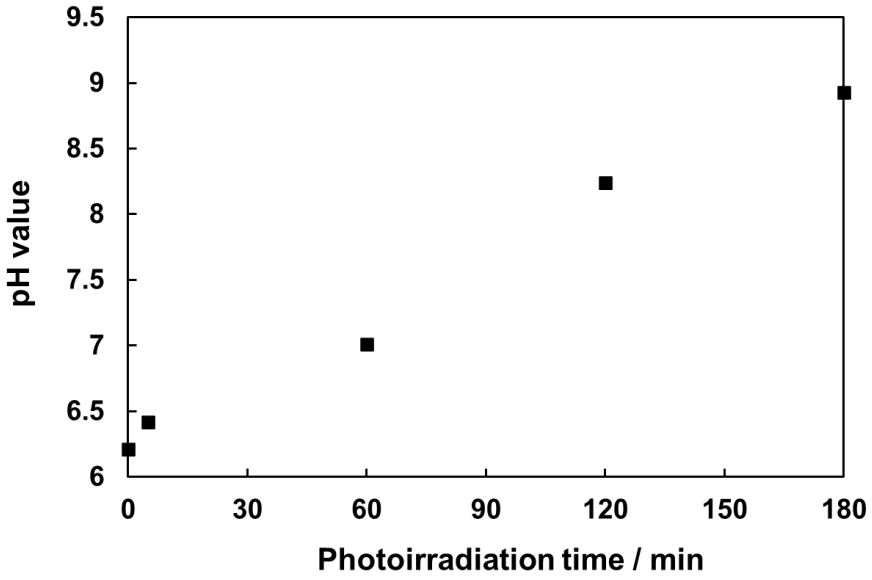

Fig. S7. The change of pH during the photocatalytic oxidation of Br^- on the Pt–$BiVO_4/WO_3$/FTO photocatalyst sheet under simulated solar light irradiation for 180 min.

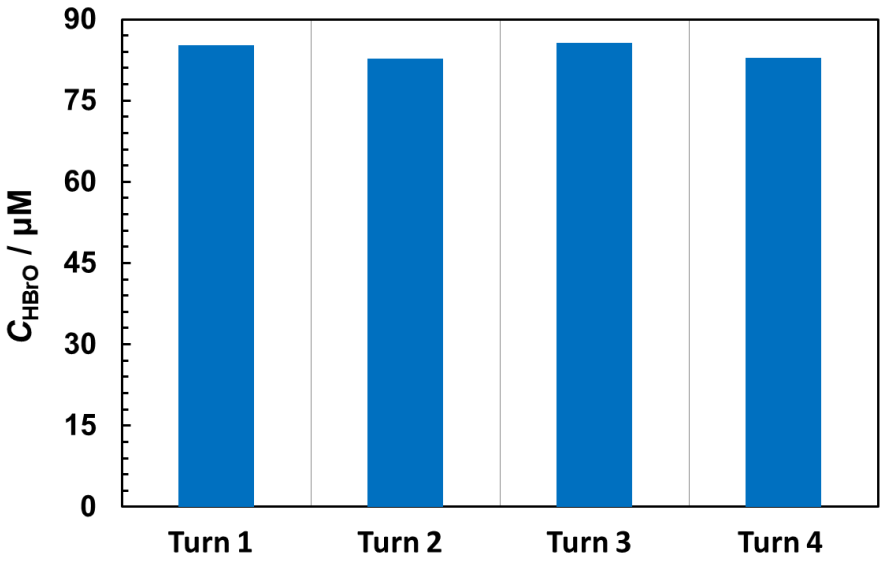

Fig. S8. Recycle test of HBrO concentration produced during the photocatalytic oxidation of Br^- over the Pt–$BiVO_4$/WO_3/FTO photocatalyst sheet (Total: 2.0 × 7.0 cm, 2.0 × 3.0 cm for $BiVO_4$/WO_3 and 2.0 × 3.0 cm for Pt film) under simulated solar light irradiation. Reaction solution: 0.5 M NaBr, 50 mL; O_2 flow rate: 1 mL min^{-1}; light source: simulated solar light (AM-1.5, 1 SUN); temperature: 303 K; photoirradiation time for recycle test: 60 min.

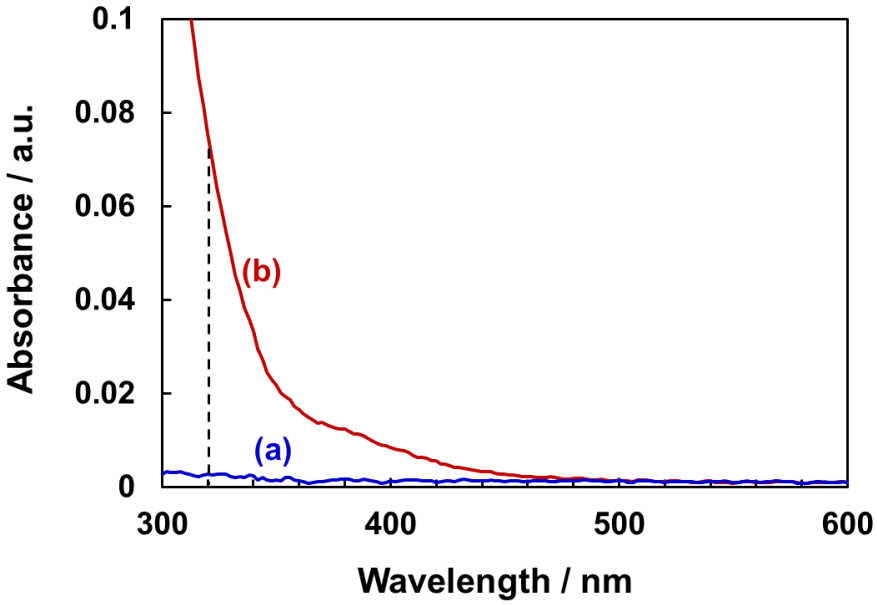

Fig. S9. Absorption spectra of (a) NaBr and (b) NaBr + HBrO aqueous solution. The concentrations of NaBr and HBrO are 0.5 M and 80 μM, respectively.

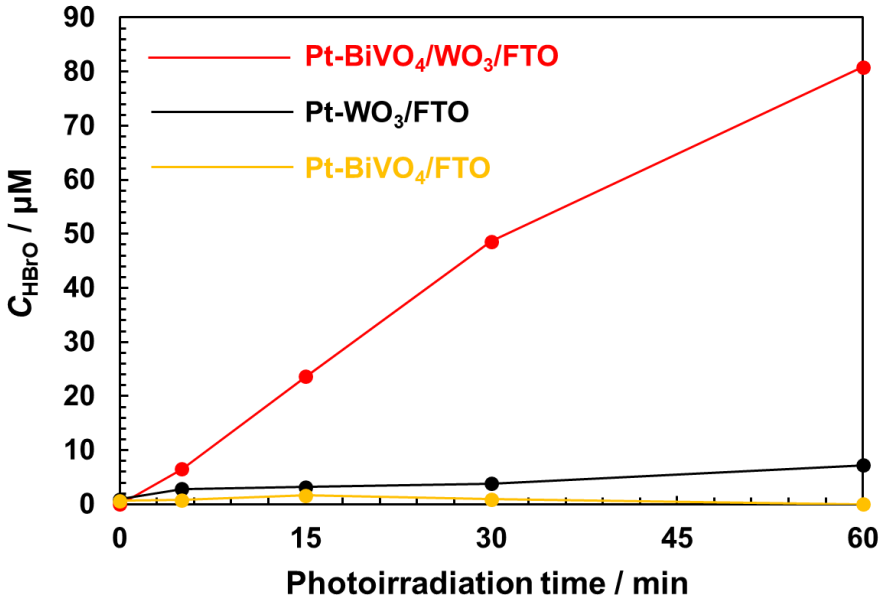

Fig. S10. HBrO concentration produced during the photocatalytic oxidation of Br^- over the Pt–$BiVO_4$/WO_3/FTO, Pt–WO_3/FTO and Pt–$BiVO_4$/FTO photocatalyst sheets under simulated solar light irradiation. Reaction solution: 0.5 M NaBr, 50 mL; O_2 flow rate: 1 mL min^{-1}; light source: simulated solar light (AM-1.5, 1 SUN); temperature: 303 K; photoirradiation time: 60 min.

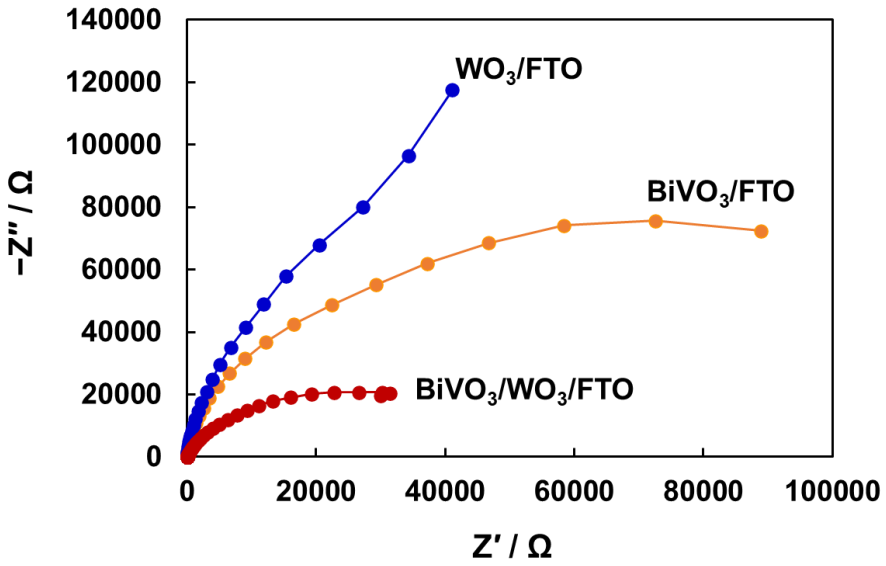

Fig. S11. Nyquist plots for WO_3/FTO, $BiVO_4$/FTO, and $BiVO_4$/WO_3/FTO photoelectrodes in 0.5 M NaBr aqueous solution under simulated solar light illumination.

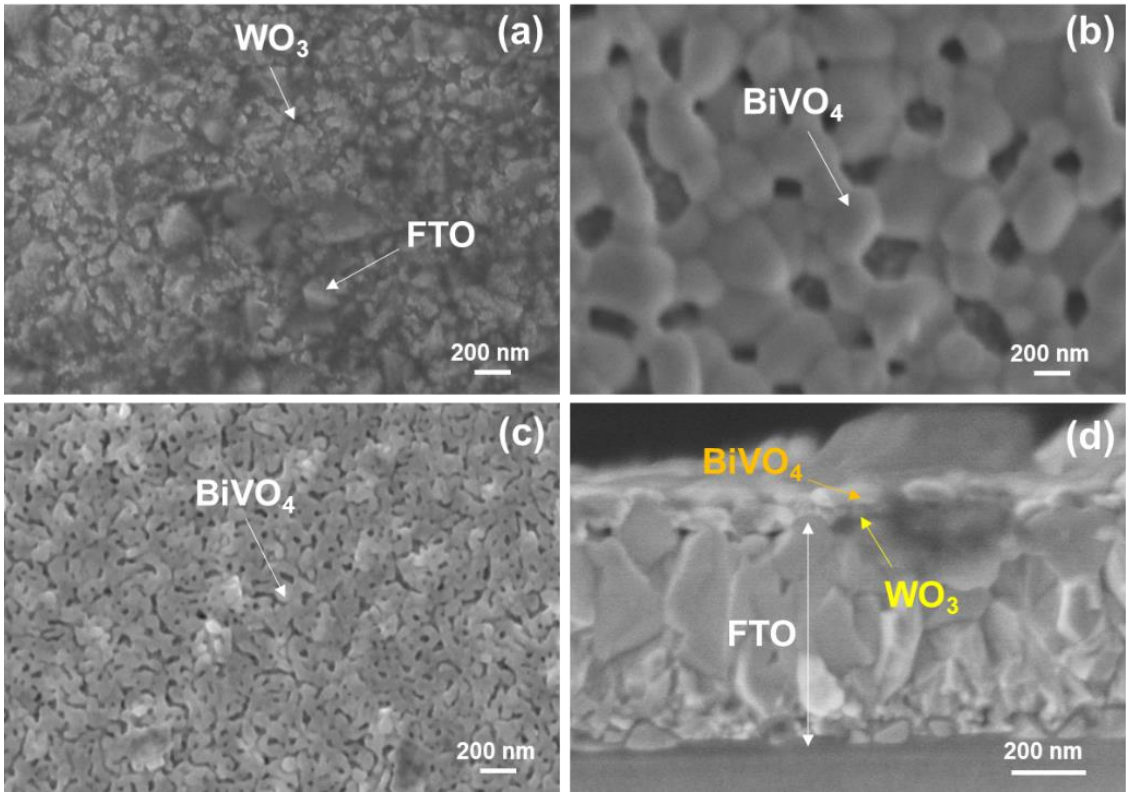

Fig. S12. SEM images of (a) WO_3/FTO, (b) $BiVO_4$/FTO and (c) $BiVO_4$/WO_3/FTO; (d) cross-section SEM image of $BiVO_4$/WO_3/FTO prepared using spin coating method.

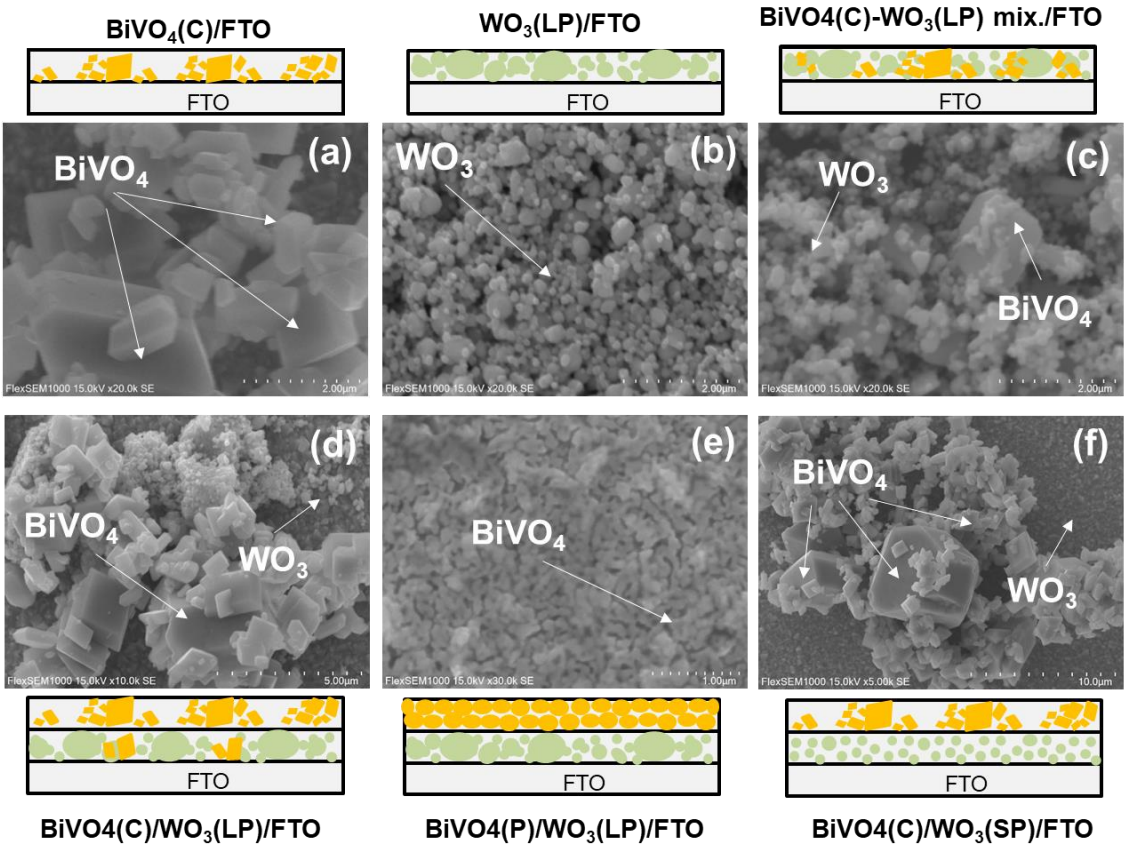

Fig. S13. Diagram and SEM images of (a) FTO loaded with $BiVO_4$ nano cubes ($BiVO_4$(C)/FTO), (b) FTO loaded with WO_3 large-size particles (WO_3(LP)/FTO), (c) FTO loaded with a mixture of $BiVO_4$ nano cubes and WO_3 large-size particles ($BiVO_4$(C)–WO_3(LP) mix/FTO), (d) FTO orderly loaded with $BiVO_4$ nano cubes and WO_3 large-size particles ($BiVO_4$(C)/WO_3(LP)/FTO), (e) FTO orderly loaded with $BiVO_4$ nano particles and WO_3 large-size particles ($BiVO_4$(P)/WO_3(LP)/FTO) and (f) FTO orderly loaded with $BiVO_4$ nano cubes and WO_3 small-size particles ($BiVO_4$(C)/WO_3(SP)/FTO).

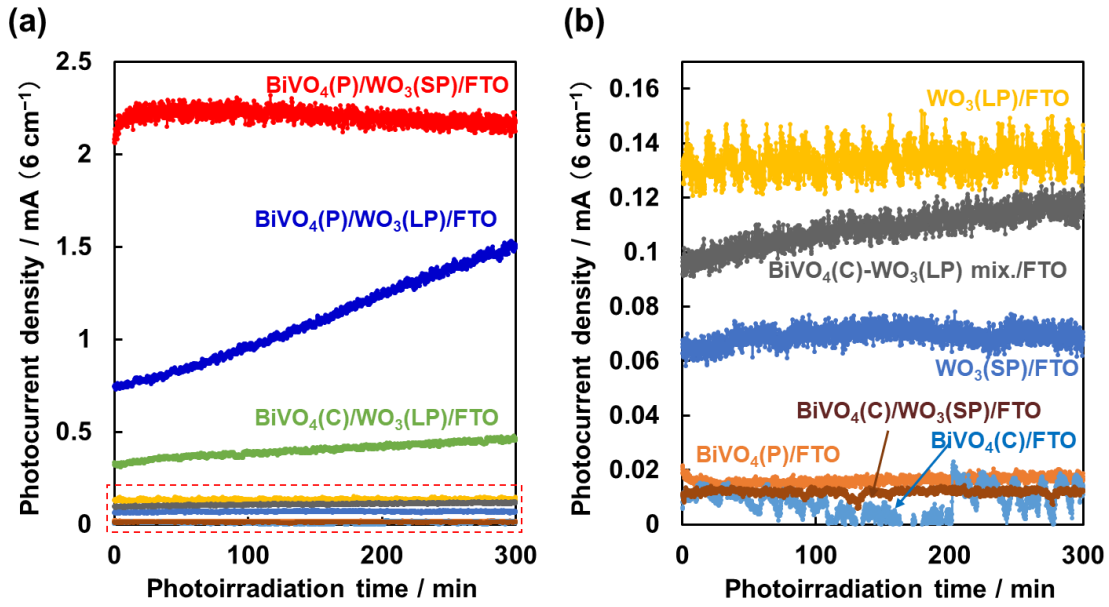

Fig. S14. *I–T* characteristic using $BiVO_4$/FTO, WO_3/FTO and $BiVO_4$/WO_3/FTO photoanodes (irradiation area: 6 cm^2) under O_2 gas bubbling and simulated solar light irradiation without any applied voltage. System: three-electrode system; electrolyte solution: 0.5 M NaBr, 50 mL; O_2 flow rate: 1 mL min^{-1}; light source: simulated solar light (AM-1.5, 1 SUN); temperature: 303 K; (b) is the enlarged image of the marked area (red box) in (a).

List of abbreviations used in Fig. S14 and Fig. 5 in main text

$BiVO_4$(P)/FTO: FTO loaded with $BiVO_4$ nanoparticles (structure: Fig. S12b).

$BiVO_4$(C)/FTO: FTO loaded with $BiVO_4$ nano cubes (structure: Fig. S13a).

WO_3(SP)/FTO: FTO loaded with WO_3 small-size nanoparticles (structure: Fig. S12a).

WO_3(LP)/FTO: FTO loaded with WO_3 large-size nanoparticles (structure: Fig. S13b).

$BiVO_4$(P)/WO_3(SP)/FTO: FTO orderly loaded with $BiVO_4$ nanoparticles and WO_3 small-size nanoparticles (structure: Fig. S12c and d).

$BiVO_4$(P)/WO_3(LP)/FTO: FTO orderly loaded with $BiVO_4$ nanoparticles and WO_3 large-size nanoparticles (structure: Fig. S13e).

$BiVO_4$(C)/WO_3(SP)/FTO: FTO orderly loaded with $BiVO_4$ nano cubes and WO_3 small-size nanoparticles (structure: Fig. S13f).

$BiVO_4$(C)–WO_3(LP) mix/FTO: FTO loaded with a mixture of $BiVO_4$ nano cubes and WO_3 large-size nanoparticles (structure: Fig. S13c).